Journal of Cell Science 109, 509-516 (1996)
Printed in Great Britain © The Company of Biologists Limited 1996
JCS4092



# Flexural rigidity of microtubules measured with the use of optical tweezers

**Harald Felgner[1,2,*], Rainer Frank[1] and Manfred Schliwa[1]**

[1]Institut für Zellbiologie, Ludwig-Maximilians-Universität, Schillerstrasse 42, D-80336 München, Germany
[2]Lehrstuhl für Biophysik E22, Technische Universität München, Garching, Germany

*Author for correspondence (e-mail: felgner@physik.tu-muenchen.de)

## SUMMARY

**The flexural rigidity of single microtubules is measured using optical tweezers. Two new methods are presented. In both the optical forces of the laser trap are used to directly manipulate microtubules grown off the ends of *Chlamydomonas* axonemes. The shapes of the microtubules are observed by video microscopy as the hydrodynamic forces of viscous flow counteract the elastic restoring forces when the microtubules are moved actively relative to the surrounding buffer medium. To determine the flexural rigidity, the bending of a microtubule is analyzed under a given velocity distribution along its length. Microtubules incubated with taxol after polymerization are measured to be more flexible than those without taxol added. On the other hand, MAPs are shown to increase microtubule stiffness.**

Key words: Flexural rigidity, Microtubule, MAP, Taxol, Optical tweezers

## INTRODUCTION

Single-beam gradient force optical traps (optical tweezers; Ashkin et al., 1986) have become an attractive new tool in cell biology. They consist of a laser beam that is highly focused by the objective lens of a standard light microscope which, at the same time, is used for observing the microscopic object. Cellular organelles or whole cells can be directly trapped, while polystyrene or glass beads can be used as 'handles' to manipulate polymers or even single molecules. The sizes of the trapped particles may vary between a fraction of the laser wavelength and some tens of micrometers. Recently, optical tweezers have been used, for example, to measure the forces exerted by single molecular motors and their step sizes (Finer et al., 1994; Kuo and Sheetz, 1993; Svoboda et al., 1993). Here we apply optical tweezers as a tool to measure directly the flexural rigidity of single microtubules.

Microtubules are polymers consisting of α- and β-tubulin subunits which form a hollow cylinder with a diameter of 24 nm (Mandelkow and Mandelkow, 1994). They are part of the eukaryotic cytoskeleton and are involved in many cellular functions such as mitosis, cell motility, and organelle transport. As skeletal proteins they contribute to the shape and polarity of cells. Different classes of proteins are known to interact with microtubules. One class, the microtubule-associated proteins (MAPs), are known to stabilize microtubules and to promote their assembly (Mandelkow and Mandelkow, 1995). The antitumor drug taxol modifies microtubule morphology in mammalian cells, and stabilizes the polymer against depolymerizing agents (Schiff et al., 1979). Whereas taxol-treated microtubules are more stable dynamically, they were found to be less rigid mechanically than untreated microtubules in two studies (Dye et al., 1993; Venier et al., 1994). Gittes et al. (1993), on the other hand, found the rigidity of taxol-stabilized microtubules to be higher than that of untreated microtubules. Knowing the flexural rigidity and its modification by different agents is essential to an understanding of the role of microtubules as cytoskeletal proteins.

The methods to measure the flexural rigidity of microtubules used so far include the observation of the changes of microtubule shape due to thermal fluctuations (Dye et al., 1993; Gittes et al., 1993; Venier et al., 1994) or hydrodynamic flow (Venier et al., 1994). In the present work, we have used optical tweezers to bend microtubules directly and derived their flexural rigidity with two new methods. The microtubules were attached at one end to axonemes glued to the coverslip. In the first method, termed RELAX, the microtubule is bent perpendicularly to its long axis with the optical tweezers only once. After switching off the laser power, the microtubule relaxes and quantitative analysis of the relaxation movement yields its flexibility. In the second method, termed WIGGLE, the optical tweezers are used to move the microtubule back and forth against the surrounding buffer. The flexural rigidity is calculated from the bending shape of the microtubule at the moment of maximum deflection. Recently, Kurachi et al. (1995) have used optical tweezers to measure microtubule rigidity. However, in contrast to their approach, we do not have to use polystyrene beads fixed to the microtubules as handles for the optical tweezers. In our methods the laser light directly grabs and bends the microtubules. The results introduce new methods into the study of the flexural rigidity of microtubules (and potentially other biopolymers) and also confirm previous findings concerning the influence of MAPs and taxol on microtubule flexibility. These methods will be useful in future studies of the influence of macromolecules on microtubule rigidity.

## MATERIALS AND METHODS

### Microtubule preparation

Microtubules were prepared from phosphocellulose-purified porcine brain tubulin according to the procedure of Shelanski et al. (1973) with modifications according to Mandelkow et al. (1985). Axonemes of *Chlamydomonas reinhardtii* were isolated as described by Witman (1986) and depleted of dynein and other endogenous proteins by salt-extraction (King et al., 1986). Axonemes were allowed to attach to polylysine-coated coverslips and incubated with purified tubulin (1 g/l) supplemented with 1 mM MgGTP for 10 minutes at 30°C. Microtubules grown this way have a length of typically 5-20 µm. Taxol (10 µM final concentration) or a fraction of microtubule-associated proteins (MAPs) isolated by phosphocellulose column chromatography (1-2 mM final concentration) were added after polymerization as desired. The buffer used was AP100 (100 mM Pipes, 2 mM $MgCl_2$, 1 mM EDTA, 1 mM EGTA, 1 mM DTT, 1 mM PMSF, 10 µg/ml trypsin inhibitor, 10 µg/ml TAME, 10 µg/ml leupeptin, 10 µg/ml pepstatin, and 10 µg/ml aprotinin, pH 6.9). The coverslip was placed on a slide and sealed with VALAP (vaseline, lanoline, and paraffin at 1:1:1). The specimen chamber formed this way had a height of approximately 15-25 µm. Observations were made at room temperature (22-25°C).

### Optical tweezers setup and image processing

The expanded, plane-polarized beam of a cw Nd:YAG laser in the $TEM_{00}$ mode (λ=1,064 nm, Spectron, Rugby, England) is coupled into an upright light microscope (Zeiss Axioskop, Oberkochen, Germany) with a 100×/1.30 objective (Zeiss Plan-NEOFLUAR) to form the optical tweezers as shown in Fig. 1. The details of the setup are as described by Felgner et al. (1995). The laser beam is fixed relative to the optical system of the microscope whereas the specimen chamber can be translated relative to the laser beam by a motorized microscope stage (Märzhäuser EK32 and MCL, Wetzlar, Germany) in three perpendicular directions. During all experiments a laser output power of 1.5 W is coupled into the epifluorescence illumination path of the microscope, which results in a power of approximately 700 mW at the specimen due to losses in the microscope optics. The specimen is observed in phase contrast mode. By placing a 4× tube (Zeiss) between microscope and Newvicon camera (Hamamatsu C2400-07, Herrsching, Germany) the microscope image is further magnified. Processing of the resulting images is performed on a Macintosh IIfx computer (Apple, Cupertino, USA) using the public domain NIH Image software (written by Wayne Rasband at the US National Institute of Health and available from ftp://zippy.nimh.nih.gov). The image processing board (PixelPipeline, Perceptics, Knoxville, USA) is used to store the video sequences recorded with an SVHS video recorder (Panasonic AG-7350, Düsseldorf, Germany) during the experiment one field at a time into the computer memory. Overall magnification of the whole optical system is that 43 nm in the object plane correspond to 1 pixel in the computer image files. Field-by-field digitization allows us to obtain a time resolution of 50 Hz. The positions of the microtubule ends and of the laser beam are tracked interactively by the experimenter. The fixed microtubule end serves as a point of reference. By calculating the other positions as differences to this point in each field, all coordinates are given in the frame of reference of the unbent microtubule. Furthermore, the position differences correct for time-base errors during still frame capture. The movements of the microscope stage are controlled via user-written algorithms integrated into the image processing software. A joystick enables fine control of the stage for the RELAX experiments where microtubules are bent only once, whereas automatic back-and-forth movement with a velocity of 10 µm/s was used for the WIGGLE method (see Results).

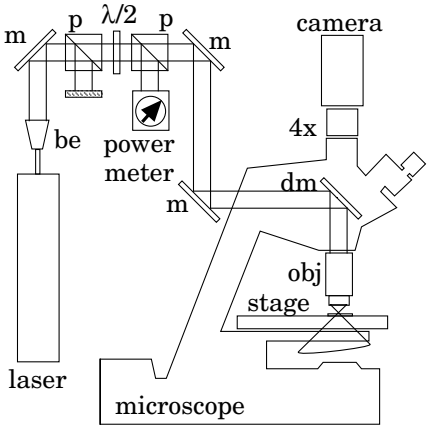


**Fig. 1**. Schematic diagram of the optical tweezers setup: be, beam expander; m, mirrors; p, polarizing beamsplitter cubes; dm, dichroic mirror; obj, objective; 4x, 4× tube. The dichroic mirror is used to reflect the infrared laser beam into the microscope objective and to transmit the image to the camera. The camera is connected to an image processing board, video recorder and monitor. The motorized stage is driven via computer control.

### Flexural rigidity theory

We consider the bending of the microtubule to be described as the linear elastic bending of a circularly symmetric rod. Then the bending moment $M$ depends linearly on the curvature $R$ of the rod (Feynman et al., 1964; Landau and Lifschitz, 1986).

$$M = EI\,\frac{1}{R} = EI\,\frac{d^2y/dx^2}{\sqrt{(1+(dy/dx)^2)^3}}\,, \tag{1}$$

with the coordinates $x$ along the unbent microtubule and $y$ orthogonal to the microtubule. $EI$ denotes the flexural rigidity. If the rod is to be considered isotropic, the flexural rigidity may be separated into the Young's modulus $E$ and the geometrical moment of inertia $I$. $E$ is a measure of the elasticity of the material of the rod, whereas $I$ depends on the geometry of the cross-section of the rod.

For small deflections, the term in the denominator is approximately equal to unity, and differentiation of equation (1) leads to the force on the microtubule per unit length $f$:

$$f = EI\,\frac{d^4y}{dx^4}\,. \tag{2}$$

The shape $y(x)$ of a bent microtubule may be derived from the differential equation (2) by succesive integration. The boundary conditions in the chosen frame of reference are for the microtubule which is fixed at the axoneme ($x$=$y$=0)

$$(y)_{x=0} = 0\,, \tag{3}$$

$$\left(\frac{dy}{dx}\right)_{x=0} = 0\,, \tag{4}$$

and for small deflections:

$$\left(\frac{d^2y}{dx^2}\right)_{x=L} = 0\,, \tag{5}$$

$$\left(\frac{d^3y}{dx^3}\right)_{x=L} = 0\,, \tag{6}$$

where $L$ is the length of the rod.

First consider a single force $F$=$F_s$ acting on the end of the microtubule in the direction $y$. The shape of the microtubule is obtained as:

$$y_s(x) = \frac{F_s L^3}{6EI}\left[-\left(\frac{x}{L}\right)^3 + 3\left(\frac{x}{L}\right)^2\right]\,, \tag{7}$$

which leads to a maximum deflection at the end of the microtubule of:

$$y_s(L) = \frac{F_s L^3}{3EI} \quad . \tag{8}$$

In an analogous way the shape of the microtubule may be calculated when it is bent by a constant force density along its length. That is the case for a microtubule in a hydrodynamic flow of constant velocity. Given a force per unit length along the microtubule of $f=f_c$, we have a bending shape of:

$$y_c(x) = \frac{f_c L^4}{24EI}\left[\left(\frac{x}{L}\right)^4 - 4\left(\frac{x}{L}\right)^3 + 6\left(\frac{x}{L}\right)^2\right] , \tag{9}$$

and a maximum deflection of:

$$y_c(L) = \frac{f_c L^4}{8EI} \quad . \tag{10}$$

Last consider a linearly increasing load along the microtubule length, $f=f_m x/L$, with the maximum force density $f_m$ at the free microtubule end. This applies to the situation when, for example, a fluid with zero velocity at the fixed microtubule end and a maximum velocity at the free end bends a microtubule. For a force density of $f=0$ at $x=0$ and $f=f_m$ at $x=L$, the corresponding results are:

$$y_l(x) = \frac{f_m L^4}{120EI}\left[\left(\frac{x}{L}\right)^5 - 10\left(\frac{x}{L}\right)^3 + 20\left(\frac{x}{L}\right)^2\right] , \tag{11}$$

and

$$y_l(L) = \frac{11 f_m L^4}{120EI} \quad . \tag{12}$$

### Hydrodynamic theory

Both the RELAX and WIGGLE experiments rely on hydrodynamic forces counterbalancing the elastic forces of the microtubules. Similar to the situation in the derivation of the microtubule shapes we may consider two cases. In the first case the force density along the microtubule is constant along its length. For a tubule moving perpendicular to its long axis through a Newtonian fluid with the velocity $v_c$, the force per unit length may be written as (Doi and Edwards, 1986):

$$f_c = \frac{4\pi\eta v_c}{\ln(L/2d)} \quad , \tag{13}$$

which, with the use of equation (10), results in a maximum deflection of the bent microtubule of:

$$y_c(L) = \frac{\pi\eta v_c L^4}{2EI\ln(L/2d)} \quad . \tag{14}$$

$\eta$ denotes the (dynamic) viscosity of the fluid and $d$ is the diameter of the microtubule.

When the fluid velocity increases linearly along the microtubule length from $v=0$ at one end to $v$ at the other end, the force per unit length is given as (Venier et al., 1994):

$$f = \frac{2\pi\eta v}{\ln(L/2d)} \quad . \tag{15}$$

Inserted into equation (12), a microtubule with zero velocity at the fixed end and a maximum velocity $v_m$ at the free end has a deflection of the free end of:

$$y_l(L) = \frac{11\pi\eta v_m L^4}{60EI\ln(L/2d)} \quad . \tag{16}$$

## RESULTS

### Flexural rigidity measurements

We have devised two procedures to measure the flexural rigidity of single microtubules that depend on different aspects of frictional hydrodynamic forces acting on a moving microtubule. These procedures are designated RELAX and WIGGLE for short and will be described in the following sections.

The single beam optical gradient trap allows us to grab objects of a refractive index higher than the refractive index of the surrounding medium at a single point. Microtubules may be directly trapped with the optical tweezers and manipulated in a direction perpendicular to their long axis. In order to be able to bend a microtubule directly with the laser tweezers, the microtubule has to be fixed. In all measurements we use demembranated flagellae of *Chlamydomonas reinhardtii* which are attached to the coverslip via poly-L-lysine. The microtubules polymerized from these axonemes parallel to the coverslip (Venier et al., 1994) may now be bent in the viewing plane of the microscope by applying a force with a component perpendicular to the microtubule.

When the laser beam is focused onto the microtubule, the microtubule is trapped in the focal point of the laser. By moving the stage and with it the axoneme and the fixed microtubule end in a direction approximately perpendicular to the long axis of the microtubule, the microtubule is bent in the focal plane of the microscope, holding it at the laser focus. In our first method, RELAX, a microtubule is captured near its free end. The laser power is switched off after bending the microtubule a certain distance (Fig. 2). During the relaxation the microtubule moves back to its straight resting position. The velocity of this movement is given by the relation between the elastic force driving back the microtubule and the hydrodynamic force of the buffer acting on the moving microtubule, which resists this movement. The movement of the microtubule through buffer is a case of low Reynolds number hydrodynamics, where inertia may be neglected relative to frictional forces. The movement of the free end of the microtubule can

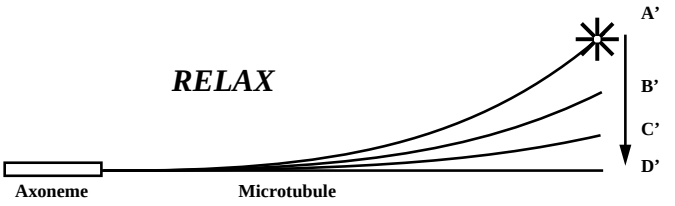


**Fig. 2.** RELAX method. In this experiment the microscope stage with the fixed axoneme is moved in the focal plane to deflect the microtubule to a position A′. When the laser is turned off the microtubule relaxes to its straight resting position D′. The position of the microtubule end is recorded during the entire relaxation from A′ via B′ and C′ to D′. The flexural rigidity is calculated from the relaxation movement.

therefore be described by a first-order differential equation which is solved by a simple exponential decay. If $y(t)$ denotes the deflection of the microtubule end, it is given by:

$$y(t) = y(0)e^{-\beta t/\gamma}, \quad (17)$$

with $y(0)$ as the maximum initial deflection and $\beta/\gamma$ as the relation of the elastic constant $\beta$ and the hydrodynamic friction constant $\gamma$. The hydrodynamic forces acting on the relaxing microtubule are given by a velocity distribution along the microtubule length reflecting the shape of the microtubule at each instant of relaxation. The relative velocity is zero at the fixed microtubule end and increases to a maximum velocity at the free, relaxing end. We approximate this velocity distribution as increasing linearly from the axoneme to the free microtubule end. Then the elastic and hydrodynamic forces are described by equations (12) and (15), respectively. Under that assumption the decay equation (17) may be rewritten as:

$$\frac{y(t)}{y(0)} = e^{-\frac{60EI\ln(L/2d)}{11\pi\eta L^4}t}, \quad (18)$$

or with the substitution $\tau$=60 ln($L$/2$d$)$t$/(11$\pi\eta L^4$):

$$\frac{y(\tau)}{y(0)} = e^{-EI\tau}. \quad (19)$$

By fitting a time series of the end positions of a relaxing microtubule to this equation, its flexural rigidity is determined.

The microtubules measured varied in length between 6.1 and 14.0 μm. A taxol microtubule of 11 μm length was maximally deflected 5 μm at its free end. In that extreme example the cosine of the corresponding initial deflection angle is 0.90. We can nevertheless justify the use of equation (2), which assumes a cosine near one. In the case of pure tubulin and MAP microtules, the microtubules were deflected less far (0.94 and 0.99 for the cosine of the angle, respectively). Fig. 3 shows a time series of the relaxation of a microtubule prepared from pure tubulin, plus its respective exponential fit to equation (18). The flexural rigidity could be directly determined from such fits for the different microtubules measured. In order to be able to compare the relaxation of different microtubules graphically, the different lengths of the microtubules used have to be taken into account. Therefore the time $t$ was transformed to a quantity $\tau$ as given above. Fig. 4 shows the result for the same microtubule as in Fig. 3 and, in addition, for a microtubule stabilized with taxol and another one stabilized with MAPs. In this way the relaxation curves can be compared directly. The ordinate is the normalized deflection, so that 1 and 0 correspond to the deflected and the relaxed position, respectively. The flexural rigidities can be directly determined as the inverse of $\tau$ at the points where the relaxation curves have reached $y(\tau)/y(0)=1/e\approx0.37$ (arrows). These three examples clearly show that taxol makes microtubules more flexible, and MAPs stiffen microtubules. A summary of all the data is presented in Table 1.

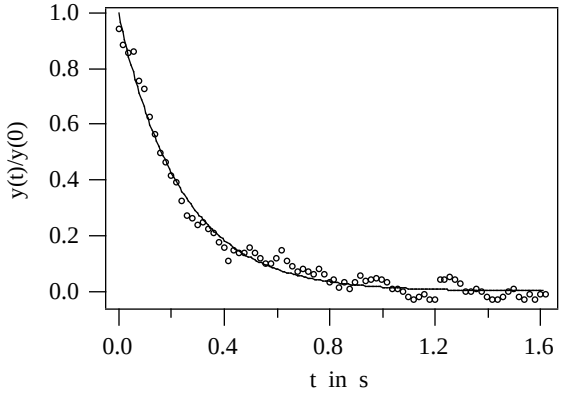


**Fig. 3.** Time series of the end of a taxol microtubule relaxing from its deflected position $y(0)$ to its resting position 0 as measured in a RELAX experiment. The circles show the measurements with a time resolution of 50 Hz, and the line represents a fit to the expected exponential decay.

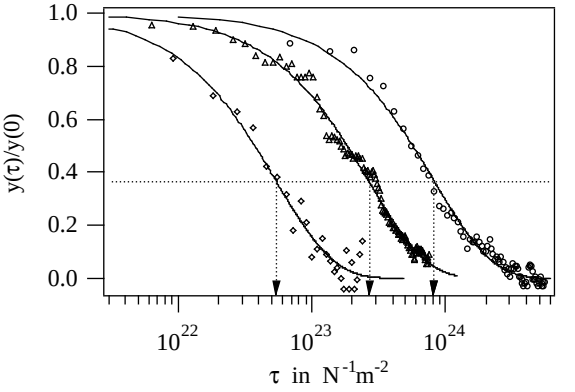


**Fig. 4.** Time series of the relaxation movements of three microtubules polymerized in taxol (circles), standard buffer (triangles), and MAPs (diamonds). The time axis of Fig. 3 was replaced by the parameter $\tau$ as described in the text to account for different microtubule lengths. The flexural rigidity of a certain microtubule can be directly taken from the graph as the inverse of the parameter $\tau$ at the position where $y(\tau)/y(0)$ has reached 0.37 (arrows). The increase in stiffness from taxol to pure and MAP microtubules can clearly be seen as a horizontal shift of the respective relaxation curves to the left. Lengths and initial deflections of the microtubles shown are: $L$=7.0 μm, $y(0)$=3.1 μm for taxol; $L$=13.2 μm, $y(0)$=4.6 μm for standard buffer; and $L$=12.0 μm, $y(0)$=1.4 μm for MAPs.

In the WIGGLE method the microtubule is held in a position somewhere between its fixed and its free end (Fig. 5). By driving the microscope stage back and forth relative to the resting laser focus, the microtubule follows a path resembling the swinging of a seesaw. Due to the hydrodynamic friction of the free end in the buffer medium, this end does not follow immediately the movement of the axoneme-fixed end. It lags behind the path a rigid rod would describe. The lag is a direct measure of the flexural rigidity of the elastic microtubule. By moving the stage with constant

**Table 1. Flexural rigidity: *EI* in $10^{-24}$ Nm$^2$ from RELAX**

| | | |
|---|---|---|
| Taxol | $n$=8 | 1.0±0.3 |
| Pure | $n$=14 | 3.7±0.8 |
| MAPs | $n$=10 | 16±3 |

Values are shown as mean ± standard deviation. $n$, number of microtubules measured.

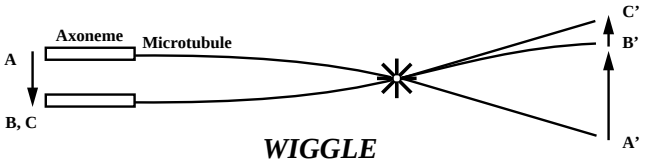


**Fig. 5.** WIGGLE method. The microscope stage with the fixed axoneme is moved back and forth in the focal plane. In the diagram one movement from position A to C is shown (left arrow). By holding the microtubule approximately in the middle, the free end of the microtubule moves antiparallel to the axoneme (right arrows). When moving the stage very slowly, this microtubule end would simply go from A′ to C′. By moving the stage with the buffer medium surrounding the microtubule faster, there acts a hydrodynamic force bending the free microtubule end against its direction of movement. Furthermore, the swinging movement around the fixed laser focus results in an additional velocity of the free microtubule end relative to the flowing buffer medium. Therefore, the free microtubule end still is deflected in a position B′ when the axoneme comes to a rest at position B. Measuring this deflection and the stage and microtubule velocities for different back and forth-movements allows to determine the flexural rigidity of the microtubule.

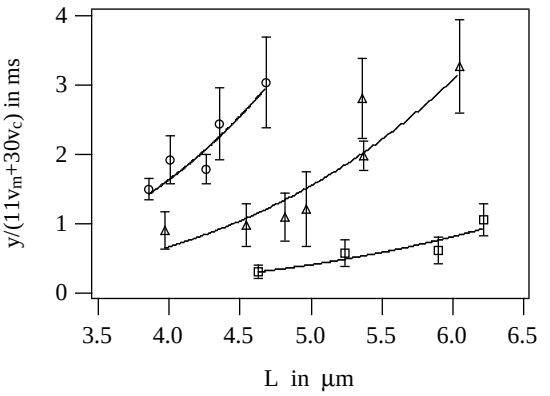


**Fig. 6.** Results from the WIGGLE experiments. The symbols are as in Fig. 4. The ordinate gives the deflection of the microtubule end relative to the sum of the weighted velocities of the microtubule end, $v_m$, and the microscope stage, $v_c$. Longer microtubules are further deflected, in accordance with equation (20). Again, the increase in stiffness from taxol to pure and MAP microtubules can clearly be deduced from the diagram.

velocity back and the same velocity forth and by resting long enough between these movements in order to have the microtubule relaxed, it is easy to extract the maximum deflection of the free microtubule end. That deflection is the distance between the position of the free end in the video frame when the microscope stage stops and the position of the resting microtubule. As stated above, during the stage movement the microtubule end is bent due to hydrodynamic frictional forces. During the seesaw movement, the total force acting on the microtubule has two components. One component stems from the buffer moving with the same constant velocity $v_c$ of the microscope stage relative to the laser beam and the microtubule. The second component stems from the free microtubule end swinging around the laser focus with zero velocity at the laser point and a maximum velocity $v_m$ at the free end. This maximum velocity can be measured as the velocity of the free microtubule end in the frame of reference of the resting camera. The velocity of the microscope stage is equal to the velocity of the axoneme. As in the case of the RELAX experiments we approximate the movement of the bent microtubule by the movement of an unbent rod, assuming that the errors are small for small deflections. Thus adding equations (14) and (16) gives a total deflection of:

$$y = \frac{\pi\eta(11v_m + 30v_c)L^4}{60EI\ln(L/2d)} . \qquad (20)$$

The deflections from different back and forth movements for one microtubule are averaged and displayed in diagrams depicting $y/(11v_m+30v_c)$ over $L$. Fitting to the expected relationship (20) yields the flexural rigidity $EI$.

The hydrodynamically relevant length of the microtubule in the WIGGLE method is the distance between the laser focus on the microtubule and its free end. This length varied between 3.8 and 6.3 μm in our experiments. The maximum deflection of a taxol microtubule of a length of 3.8 μm did not exceed 0.5 μm, resulting in a cosine of the deflection angle of 0.99, near unity, justifying the assumption of small deflections in equation (2). Fig. 6 shows the measurements of the deflections for microtubules prepared from pure tubulin, in a mixture of MAPs, and in taxol under the same conditions as for the RELAX method. To be able to compare different microtubules, the deflections are normalized to the weighted velocities of the free microtubule end and the microscope stage, as these different microtubules are not trapped at exactly the same distance from their free ends. The errors of the flexural rigidity were calculated from the nonlinear least-squares fits as asymptotic standard errors, where the single points in Fig. 6 were weighted by their inverse standard deviations from Gaussian error propagation (error bars). Johnson (1994) states that the asymptotic standard errors usually underestimate the actual confidence limits. The results are summarized in Table 2. As in the case of the RELAX experiments, microtubule rigidity clearly increases from taxol microtubules over pure microtubules to MAP microtubules.

By using an approach similar to the RELAX procedure, it is possible to estimate the optical forces exerted on a single microtubule by the laser. When not switching off the laser power at a certain deflection, the microtubule will finally escape from the trap. At that moment the flexural restoring force is equal to the maximum lateral optical force of the laser trap. As this force acts at only one point of the microtubule near the end, the deflection is described by equation (8). In that case $L$ is denoting the distance of the fixed microtubule end to the laser focus. By insertion of the flexural rigidity from the RELAX experiments for microtubules under different conditions, we may obtain the optical forces on these micro-

**Table 2. Flexural rigidity: $EI$ in $10^{-24}$ Nm$^2$ from WIGGLE**

| | | |
|---|---|---|
| Taxol | $n$=5 | 1.9±0.1 |
| Pure | $n$=7 | 4.7±0.4 |
| MAPs | $n$=4 | 18±3 |

Values are shown as fit parameter ± assymptotic standard errors. $n$, number of microtubules measured.

tubules. We found in preliminary experiments with 6 untreated microtubules a value of (42±12) *fN* at a laser power of approximately 700 mW.

## Factors affecting the measurements

### Temperature

The proportion of the laser power which is absorbed in the buffer and microtubule leads to a rise of the temperature in the specimen chamber. The temperature was measured using a NTC resistor as described by Felgner (1993) and shown to rise no more than 2°C for the laser powers used here.

### Physical damage

An infrared laser was used, because it has been shown to have the least damaging influences on biological specimens (Ashkin and Dziedzic, 1987). Direct damage of the manipulated microtubules was not observed during the time period required for both the RELAX and WIGGLE procedures (1-5 seconds). Visible damage (breaking) may occur after 1-2 minutes of continuous trapping of a microtubule.

### Dynamic instability

Brain microtubules prepared from pure tubulin undergo dynamic instability and either grow or shrink at rates of approximately 3 μm/minute and 25 μm/minute, respectively (Walker et al., 1988). Since microtubule length is an important parameter in the determination of flexural rigidity, microtubule dynamic instability may affect the measurements. However, since an experiment using either the RELAX or the WIGGLE method does not last longer than 5 seconds, microtubule growth during the experiment introduces an error of no more than 10% for a microtubule of approximately 10 μm length. Taxol and MAP microtubules are even less affected. Shrinking microtubules were not used for the analysis.

### Protofilament number

The number of protofilaments of microtubules polymerized off the ends of flagellar axonemes is 13 for A-microtubules and 14 for B-microtubules (Scheele et al., 1982). Assuming the same Young's modulus $E$ for microtubules with 13 or 14 protofilaments, the flexural rigidity $EI$ of a 14mer would be higher because of an increased geometric moment of inertia $I$. As $I$ depends on the number of protofilaments by the third power (Gittes et al., 1993), the resulting change in the diameter of a microtubule would change the flexural rigidity by no more than 25%. Given the experimental errors, it would not be possible to distinguish between the two classes of microtubules.

### MAP binding to the microtubules

The MAPs binding to the microtubules have an assembly domain that binds along the length of a microtubule and a projection domain that extends from the microtubule surface (Mandelkow and Mandelkow, 1995). By reaching out into the buffer, these projection domains could increase the hydrodynamic radius of the microtubules compared to untreated or taxol-treated microtubules. As the diameter enters the hydrodynamic equations (13) and (15) together with the much greater microtubule length inside the logarithm, the effect of the underestimation of the rigidity by taking the standard microtubule diameter is minor. An assumed doubling of the hydrodynamic radius for the MAP microtubules would lead to an underestimation of 20% in the worst case of a short microtubule of 4 μm length.

### Proximity of the coverslip

A potential source of uncertainty is the fact that the microtubules are close to the coverslip surface. Venier et al. (1994) determined that microtubules attached to axonemes are constrained in a layer 0.4 μm thick centered at a distance of about 0.3 μm from the glass surface. The hydrodynamic theory described above and summarized in equations (13) and (15) assumes that there are no boundaries present in finite distances from the moving cylinder. Even for this case there is no consensus in the literature about the exact hydrodynamic forces on a cylinder (Cox, 1970; Doi and Edwards, 1986; Hunt et al., 1994; Landau and Lifschitz, 1991; Venier et al., 1994). Hunt et al. (1994) give in their appendix A a detailed description of several correction factors for unbounded cylinders of finite length. In the same publication the authors present a different expression for the force on a microtubule moving near a coverslip. As our microtubules are at a much greater distance from the coverslip than their microtubules used in a kinesin gliding assay (10 nm), the coverslip has a distinctly lesser influence on the microtubule movement in our case. Nevertheless, using the equation (A2) for the frictional constant from Hunt et al. (1994), equation (13) would be off by a factor of 1.4 and 2.0 for distances of 300 and 100 nm between microtubule and coverslip, respectively. That means that our values of the flexural rigidity would be too low by a factor of two maximum, given the range of distances from the coverslip suggested by Venier et al. (1994). However, the relative values of the stiffness of microtubules prepared under different experimental conditions would remain unchanged upon such a correction. As the influence of other factors, such as the finite length of the microtubule, on the hydrodynamics remain difficult to resolve theoretically, resulting in end correction terms for the free and the fixed microtubule ends in equations (13) and (15) and also in the expressions of Hunt et al. (1994), we refrained from correcting our values for the proximity of the coverslip surface. To emphasize this point once again, the methods described are nevertheless very sensitive to relative changes in microtubule rigidity.

## DISCUSSION

Using three different types of microtubules (pure tubulin microtubules, microtubules bound with MAPs, and taxol-treated microtubules) as examples, we have devised and tested two different procedures to determine the flexural rigidity of single microtubules using optical tweezers. In contrast to a recently described procedure also employing optical tweezers (Kurachi et al., 1995), our methods do not require the attachment of refractive beads to the microtubule. In addition, our methods to measure flexural rigidities do not directly depend on the absolute light forces (as long as the laser power is high enough to hold or bend a microtubule). The RELAX method is particularly convenient to apply using the tools and mathematical procedures described here and yields useful data relatively rapidly.

The two procedures described here are both based on a forced, temporary deflection of a microtubule, followed by its

return movement to a resting state. The optical tweezers are used as an instrument of nanomanipulation, and determination of the flexural rigidity of microtubules is independent of the precise knowledge of the force applied by the laser trap. The two methods are comparable, but independent. They yield values for the flexural rigidity of microtubules that are in reasonably good agreement with each other and with measurements based on other published procedures. For example, using hydrodynamic flow and thermal fluctuations, Venier et al. (1994) determined the flexural rigidity of microtubules to be 8.5 and $4.6\times10^{-24}$ $Nm^2$ (corrected by a missing factor of two in the original work as described by Venier et al., 1995), respectively. Thus, their result from hydrodynamic flow and our results differ by a factor of approximately 2, while their corrected result from thermal fluctuations agrees quite well with ours. The flexural rigidity of taxol-treated microtubules is found to be approximately $2.5\times10^{-24}$ $Nm^2$ by Venier et al. (1994, 1995) and $5.9\times10^{-24}$ $Nm^2$ by Kurachi et al. (1995) (for a comparable length of microtubules; see discussion of length dependency below). Thus, the thermodynamic procedure of Venier et al. (1994, 1995) determines taxol-treated microtubules to be more flexible than untreated microtubules by a factor of 2, in agreement with our findings. The results of Dye et al. (1993) are a factor of 2-3 lower than ours for untreated microtubules, and a factor of 10 for taxol microtubules. So their measurements show an even stronger decrease in the microtubule stiffness after taxol treatment. Kurachi et al. (1995) also measured the rigidity of MAP-stabilized microtubules to be $35\times10^{-24}$ $Nm^2$ (for a comparable length), finding them to be a factor of 6-7 stiffer than taxol-treated microtubules. We find an increase of stiffness from taxol-treated microtubules to MAP-stabilized microtubules by factors of 16 and 9 for RELAX and WIGGLE, respectively.

Thus, even though some differences in the absolute magnitude of the flexural rigidity of microtubules as determined in the different laboratories mentioned exist, the consensus seems to emerge that taxol makes microtubules more flexible and MAPs increase their rigidity. In contrast to that, recently published results by Mickey and Howard (1995) confirm earlier work from the same group (Gittes et al., 1993) that taxol-treated microtubules are stiffer than untreated microtubules. Whereas their finding that microtubules treated with tau protein have a flexural rigidity of $34\times10^{-24}$ $Nm^2$ agrees well with our findings (unpublished results), we cannot see the stiffening effect in our preparation of taxol microtubules. Regardless of the fact that different procedures to determine flexural rigidity might lead to different absolute values due to as yet unknown systematic errors, simple visual inspection already reveals the much more flexible appearence of taxol treated microtubules in our preparations. This same observation was made by other groups who determined taxol to reduce microtubule stiffness (Dye et al., 1993; Kurachi et al., 1995; Venier et al., 1994). It is conceivable, therefore, that the taxol microtubules prepared from different groups might not be comparable due to structural differences. For example, taxol might exert different effects on microtubules with different protofilament numbers, as obtained by polymerization in solution or off axonemes (Arnal and Wade, 1995). According to Venier et al. (1994), the increase in the stiffness of taxol-treated microtubules determined by Gittes et al. (1993) is due to constraints introduced by the methods used in this study. On the other hand, Mickey and Howard (1995) point out potentially serious flaws in the work of the other groups. According to them the measurements of Dye et al. (1993) were possibly dominated by digitization errors, and the two methods used by Venier et al. (1994) would not agree very well with each other after correcting the thermal fluctuation results with the missing factor (Venier et al., 1995). Furthermore, the hydrodynamic equations would not fully account for the nearby surface. The same point of criticism might apply to the work presented here. As described above, the use of equations (13) and (15) potentially underestimates the absolute value of the flexural rigidity. Nevertheless, despite the differences and possible errors in the absolute magnitudes of the flexural rigidity, our work shows that taxol-treated microtubules are more flexible than untreated microtubules and that MAP-treated microtubules are stiffer than untreated microtubules under the experimental conditions used here.

An unexpected result of the work of Kurachi et al. (1995) is their finding that the flexural rigidity of a longer microtubule is higher than that of a shorter one. Our results from both methods described here cannot serve to confirm such a length dependence. Their methods and their results are somehow inconsistant with each other, as they first do assume a constant rigidity along the length of a single microtubule in their method to determine the stiffness, and with that assumption they then get different rigidities for microtubules of different lengths. Furthermore, the flexural rigidity should be a constant, by definition, for a rod-like polymer which is symmetric under translation along its long axis.

Using the methods described here, we are now in a position to determine the influence of other agents or microtubule-binding proteins on the mechanical properties of these important cytoskeletal polymers.

This work was supported by the Deutsche Forschungsgemeinschaft (SFB 266) and a grant from the Friedrich-Baur-Stiftung. The idea for the procedures used in this study was inspired by initial discussions with Arthur Ashkin.

## REFERENCES

**Arnal, I. and Wade, R. H.** (1995). How does taxol stabilize microtubules? *Curr. Biol.* **5**, 900-908.

**Ashkin, A. and Dziedzic, J. M.** (1987). Optical trapping and manipulation of viruses and bacteria. *Science* **235**, 1517-1520.

**Ashkin, A., Dziedzic, J. M., Bjorkholm, J. E. and Chu, S.** (1986). Observation of a single-beam gradient force optical trap for dielectric particles. *Opt. Lett.* **11**, 288-290.

**Cox, R. G.** (1970). The motion of long slender bodies in a viscous fluid. I: General theory. *J. Fluid Mech.* **44**, 791-810.

**Doi, M. and Edwards, S.** (1986). *The Theory of Polymer Dynamics*. Clarendon, Oxford.

**Dye, R. B., Fink, S. P. and Williams, R. C.** (1993). Taxol-induced flexibility of microtubules and its reversal by MAP-2 and tau. *J. Biol. Chem.* **268**, 6847-6850.

**Felgner, H.** (1993). Die LaserPinzette: Charakterisierung und Eichung der Lichtkräfte einer optischen Einstrahl-Falle im Lichtmikroskop. MS thesis, Technische Universität München.

**Felgner, H., Müller, O. and Schliwa, M.** (1995). Calibration of light forces in optical tweeezers. *Appl. Opt.* **34**, 977-982.

**Feynman, R. P., Leighton, R. B. and Sands, M.** (1964). The Feynman Lectures on Physics II. Addison-Wesley, Reading, MA.

**Finer, J. T., Simmons, R. M. and Spudich, J. A.** (1994). Single myosin molecule mechanics: piconewton forces and nanometre steps. *Nature* **368**, 113-119.

**Gittes, F., Mickey, B., Nettleton, J. and Howard, J.** (1993). Flexural rigidity of microtubules and actin filaments measured from thermal fluctuations in shape. *J. Cell Biol.* **120**, 923-934.

**Hunt, A. J., Gittes, F. and Howard, J.** (1994). The force exerted by a single kinesin molecule against a viscous load. *Biophys. J.* **67**, 766-781.

**Johnson, M. L.** (1994). Use of least-squares techniques in biochemistry. *Meth. Enzymol.* **240**, 1-22.

**King, S. M., Otter, T. and Witman, G. B.** (1986). Purification and characterization of Chlamydomonas flagellar dyneins. *Meth. Enzymol.* **134**, 291-306.

**Kuo, S. C. and Sheetz, M. P.** (1993). Force of single kinesin molecules measured with optical tweezers. *Science* **260**, 232-234.

**Kurachi, M., Hoshi, M. and Tashiro, H.** (1995). Buckling of a single microtubule by optical trapping forces: direct measurement of microtubule rigidity. *Cell Motil. Cytoskel.* **30**, 221-228.

**Landau, L. D. and Lifschitz, E. M.** (1986). *Theory of Elasticity*, 3rd edn. Pergamon Press, Oxford.

**Landau, L. D. and Lifschitz, E. M.** (1991). *Hydrodynamik, 5*. Aufl. Akademie Verlag, Berlin.

**Mandelkow, E. and Mandelkow, E.-M.** (1994). Microtubule structure. *Curr. Opinion Struct. Biol.* **4**, 171-179.

**Mandelkow, E. and Mandelkow, E.-M.** (1995). Microtubules and microtubule-associated proteins. *Curr. Opin. Cell Biol.* **7**, 72-81.

**Mandelkow, E.-M., Hermann, M. and Rühl, U.** (1985). Tubulin domains probed by limited protolysis and subunit-specific antibodies. *J. Mol. Biol.* **185**, 311-327.

**Mickey, B. and Howard, J.** (1995). Rigidity of microtubules is increased by stabilizing agents. *J. Cell Biol.* **130**, 909-917.

**Scheele, R. B., Bergen, L. G. and Borisy, G. G.** (1982). Control of the structural fidelity of microtubules by initiation sites. *J. Mol. Biol.* **154**, 485-500.

**Schiff, P. B., Fant, J. and Horwitz, S. B.** (1979). Promotion of microtubule assembly in vitro by taxol. *Nature* **277**, 665-667.

**Shelanski, M. L., Gaskin, F. and Cantor, C. R.** (1973). Assembly of microtubules in the absence of added nucleotides. *Proc. Nat. Acad. Sci. USA* **70**, 765-768.

**Svoboda, K., Schmidt, C. F., Schnapp, B. J. and Block, S. M.** (1993). Direct observation of kinesin stepping by optical trapping interferometry. *Nature* **365**, 721-727.

**Venier, P., Maggs, A. C., Carlier, M.-F. and Pantaloni, D.** (1994). Analysis of microtubule rigidity using hydrodynamic flow and thermal fluctuations. *J. Biol. Chem.* **269**, 13353-13360.

**Venier, P., Maggs, A. C., Carlier, M.-F. and Pantaloni, D.** (1995). Analysis of microtubule rigidity using hydrodynamic flow and thermal fluctuations. *J. Biol. Chem.* **270**, 17056.

**Walker, R. A., O'Brian, E. T., Pryer, N. K., Soboeiro, M. F., Voter, W. A., Erickson, H. P. and Salmon, E. D.** (1988). Dynamic instability of individual microtubules analyzed by video light microscopyrate constants and transition frequencies. *J. Cell Biol.* **107**, 1437-1448.

**Witman, G. B.** (1986). Isolation of Chlamydomonas flagella and flagellar axonemes. *Meth. Enzymol.* **134**, 280-290.

(Received 19 September 1995 - Accepted 16 November 1995)